FINAL REPORT

to the

NATIONAL AERONAUTICS AND SPACE ADMINISTRATION

George C. Marshall Space Flight Center
Marshall Space Flight Center, Alabama 35812

for

CONTRACT NO. NAS8-24668

TITLE OF RESEARCH:

"Astronomical X-Ray Polarimetry Program-Definition Phase" Study

SUBMITTED BY:

Columbia Astrophysics Laboratory
Department of Astronomy - Department of Physics
Columbia University
New York, New York 10027

R. Novick
Principal Investigator

March 1971

TABLE OF CONTENTS

I. INTRODUCTION

The proposed research under contract NAS8-24668 involved the study, design, and testing of mosaic crystal x-ray polarimeters and spectrometers. Particular emphasis was placed on the development of such instruments for the eventual use in the High Energy Astronomical Observatories (HEAO) to be flown by NASA in the mid 1970's.

The work described in the following pages developed as a natural extension of the program of research in the Columbia Astrophysics Laboratory. From this study, the use of mosaic crystals for celestial x-ray polarimetry and spectroscopy and their application in a large orbiting x-ray observatory were developed, and the following conclusions were drawn:

1. That certain crystalline materials such as graphite, lithium hydride, and tungsten disulphide in their mosaic form are ideally suited for significant celestial x-ray polarimetry.

2. That such crystals, particularly lithium hydride, when coupled with an x-ray telescope to form an objective crystal spectrometer, result in a device that combines the highest possible spectral resolution with the highest possible efficiency of a scanning spectrometer for the study of the broad spectral lines expected from high-temperature stellar sources.

3. That such crystals can be usefully employed in a slitless spectrometer in those situations where the time of observation per resolution element is limited such as in a rocket with two- or three-degree pointing accuracy or in the wheel section of an OSO or similar-type satellite.

4. That crystals of tungsten disulphide, though not currently available, could be created by the same or similar methods as the graphite crystals, namely, pyrolytic deposition followed by compression under high temperatures (Union Carbide). A subcontract with Union Carbide Corporation was negotiated to prepare samples of this material.

In order to develop and demonstrate these concepts, the following instruments were constructed:

1. A highly efficient flight prototype of a graphite crystal polarimeter to be used in the focal plane of a grazing-incidence x-ray telescope. This polarimeter placed at the focus of an x-ray telescope of 1000-cm^2 effective area could detect polarization of less than 5% from Crab-nebula-strength sources in 1000 seconds of observation time.

2. Two large-area (150 square inches each) graphite crystal spectrometers, which were flown successfully in a sounding rocket (KP330) launched on April 24, 1970.

3. A laboratory objective crystal spectrometer employing graphite crystals, which to date has demonstrated a resolution of better than 12 arc min at 2.6 keV.

4. Four large-area focusing graphite polarimeters, which are to be flown in an Aerobee-350 (17.09 U.G.) in February, 1971.

In addition to the work outlined above, we have, through a subcontract to Union Carbide Corporation, also realized the development of a process for producing large areas of the mosaic form of tungsten disulphide.

II. MATERIAL STUDIES

Highly imperfect or "mosaic" crystals can be considered to consist of microscopic perfect crystallets (domains), each slightly misaligned with respect to one another. Each domain then satiafies the Bragg condition at a slightly different energy for parallel incident radiation. The total intensity reflected by the crystal is simply the sum of the intensities reflected by the individual domains. The commonly used measure of this property is the integrated reflectivity. Crystals with high integrated reflectivity insure that the largest possible fraction of parallel continuum radiation, such as that encountered in stellar x-ray sources, will be coherently scattered.

The first phase of our program established which mosaic crystals had the largest integrated reflectivities. An examination of the theoretical formula showed that the integrated reflectivity is maximized for those crystals with (a) a large value of the ratio of differential coherent to absorption cross section, and (b) dense, widely separated planes. Computer calculations were performed for many crystals that seemed to satisfy either or both of the above conditions. A sample of the results of these calculations is shown in Table I. The mosaic forms of graphite, lithium hydride, and tungsten disulphide were found to have the highest value of the integrated reflectivity.

A. Mosaic Graphite

A test facility was constructed and used for the study of the properties of a large sample of commercially produced (Union Carbide) mosaic graphite crystals. This work led to a detailed understanding of

Table I. Integrated Reflectivity at 45° Incidence for Mosaic Forms of Various Crystals*

	E	I. R. x 10^4
Kalonite	1.19	1.6
Fe_4N	4.64	5.7
Mica	8.80	0.2
Graphite	2.62	12.
WSe_2	1.35	14.
PET	2.0	4.3
MO	5.58	1.6
W	5.55	3.0
TaC	3.94	3.7
AgCl	3.16	4.6
WS_2	1.41	16.
MOS_2	1.43	7.8
InOCL	1.09	3.4
Calcite	5.42	3.7
LiF	4.37	5.2
LiH	4.30	17.

*Absorption coefficients are from the tables of Leroux, J., The Encyclopedia of X-Rays and Gamma Rays, Ed., G. L. Clark, Reinhold Publishing Corp., New York (1963), p. 9. The atomic structure factors are from Hanson et al., Acta Cryst. (1964) 18, 1040. The crystal structure factors were calculated from the atomic locations in Wyckoff's tables.

the specification of the properties of these crystals for use in x-ray polarimeters and spectrometers. Studies were also made of techniques to improve the integrated intensity of the graphite crystals.

The integrated reflectivity of the graphite crystals produced by Union Carbide was not necessarily identical for crystals with the same mosaic spread. The integrated reflectivity depended on the production process used. In particular, the integrated reflectivity (for a given mosaic spread) was found to be greater for those crystals produced at low temperatures and high pressures. Furthermore, the mosaic spread of the entire crystal is typically 30 to 50 percent greater than the value specified by Union Carbide on the basis of testing less than one percent of the total area of the 1-in.-square crystals. Therefore, specification of the mosaic spread is not sufficient for determining the expected performance of these crystals.

It was found that some of the crystals produced by Union Carbide exhibited integrated reflectivity as high as 12×10^{-4}, but many of the crystals had lower reflectivities. By using various techniques for torturing the crystal, such as grinding, heating, and cooling, we could improve the poorer crystals to the above value, but in no case were we able to obtain a reflectivity higher than 12×10^{-4}. Calculations based on the atomic factors given by Leroux[1] indicate that a 50% higher reflectivity is theoretically attainable. However, the value of 12×10^{-4} is found to be in agreement with the theoretical limit calculated from the more recent work of Doyle and Turner.[2]

---

[1]Leroux, J., 1963, The Encylopedia of X-Rays and Gamma Rays, ed., George L. Clark (New York: Reinhold Publishing Co.).

[2]Doyle, P. A. and Turner, P. S., 1968, Acta Cryst. A24, 390.

The results of our experiments to improve the integrated reflectivity of the graphite crystals are shown in Table II. The majority of the samples used in these experiments were cleaved or stripped from a thick crystal with 3.3° mosaic spread. In order to improve integrated reflectivity, one has to minimize the domain size to reduce primary extinction and to misalign the domains to reduce secondary extinction. The techniques used in these experiments included:

Hammering. The surface of the crystal was repeatedly struck with a hammer.

Acid treatment. The crystals were bathed at room temperature in either HCl or a mixture of 85% H_2SO_4 and 15% HNO_3.

Heat treatment. The crystals were repeatedly immersed first in liquid N_2, then in warm water; or first in molten solder, then in ice water.

Sandblasting.

Flight tape. The sticky side of a heavy-duty tape was used to remove a thin layer from the surface of the crystal. The section of crystal left on the tape could then be easily twisted, bent, etc. in order to perturb the crystal structure.

Stripping. Thin ($\leq$ 0.005-in.) strips of crystal were removed from the surface by placing a piece of Scotch cellulose tape on the edge of the crystal and pulling back. This process of peeling graphite from graphite produces striations in the peeled material.

Pressure. Both strips and cleaved sections of crystal were subjected to forces ranging from 2000 to 200,000 lbs.

Table II. Summary of Experiments to Improve the Integrated Reflectivity of Graphite

Method	Mosaic Spread (degrees)	Peak Reflectivity (per cent)	Integrated Reflectivity ($\times 10^4$)	Comment (B.T. - Before Treatment) (A.T. - After Treatment)
Hammering	4.5	0.78	7.0	B.T.
	3.9	0.98	8.0	A.T.
Acid	1.7	0.98	4.7	B.T. (HCL)
	2.1	1.05	5.8	A.T.
	2.3	0.85	4.2	B.T. 85% H_2SO_4; HNO_3
	3.2	0.65	4.2	A.T.
Temperature	3.9	0.98	8.0	B.T. Liquid $N_2 \leftrightarrow H_2O$
	5.0	0.50	4.7	A.T.
	4.8	1.1	10.1	B.T. "Strip"
	4.0	1.0	8.2	A.T.
	6.0	0.45	4.7	B.T. Molten solder-ice water
	6.0	0.38	3.8	A.T.
Sand-blasting	1.4	1.50	4.7	B.T.
	1.5	0.98	3.8	A.T.
	2.7	0.70	4.3	B.T. Sample protected during process
	3.0	0.78	4.9	A.T.
Flight tape	2.3	0.85	4.2	B.T. (Typical only)
	1.1	1.85	6.2	A.T.
	1.9	1.55	6.9	A.T.
Strips	2.3	0.85	4.2	B.T. (Typical)
			9.6	A.T. 10 strips <.001" together
			10.0	A.T. 3 strips each 1-2 mil
			10.1	A.T.
			8.6	A.T.
	5.3	1.0	10.1	A.T.
	4.8	1.1	10.1	A.T.
Pressure			9.3	A.T. strips at 2000 lb
			9.8	A.T. 3 strips at 50K lb
	3.9	0.7	4.8	B.T. Cleaved sect.
	2.6	1.7	9.3	A.T. 200K lb
	2.5	1.0	5.8	B.T.
	2.3	1.5	7.3	A.T. 200K lb

Table II (cont'd)

Method	Mosaic Spread (degrees)	Peak Reflectivity (per cent)	Integrated Reflectivity ($X\ 10^4$)	Comment (B.T. - Before Treatment) (A.T. - After Treatment)
Pressure (cont'd)	6.3	0.65	6.9	B.T.
	2.5	1.85	8.7	A.T. 100K lb
	7.5	0.72	8.7	B.T.
	5.1	1.00	9.0	A.T. 45K lb
	4.0	0.74	6.0	B.T.
	2.8	1.55	9.6	A.T. 45K lb
	1.9	2.15	9.6	A.T. 50K lb
	1.5	1.75	6.9	A.T. 200K lb
	2.5	1.53	9.3	A.T. 2K lb
	2.0	1.70	7.8	A.T. 100K lb

The last two methods described above consistently improved the integrated intensity of samples whose initial value of this property was less than 1×10^{-3}. While the stripping technique worked very well on poor samples, those crystals produced under high pressures by Union Carbide have a much more brittle texture and are impossible to "strip." However, the high-pressure samples test typically to 9×10^{-4} or better without treatment.

Under the pressure treatment, poor samples improved provided that the applied force was not greater than about 50,000 lbs. As one would expect, secondary extinction became a problem in samples subjected to very high pressures. Finally, pressing the striated strips or samples of 0.8° material, which tested initially to better than 1×10^{-3}, produced no improvement in their integrated intensity.

Almost all of the measurements discussed above were performed with a Norelco Universal Vacuum X-Ray Spectrometer (type 52530). The x-ray beam produced by this apparatus is only capable of sampling a fraction of the 1 in. by 1 in. surface of the graphite crystals (1/32 sq. in.). In order to test the entire crystal with a well-collimated beam (better than 0.1°), a test facility was constructed incorporating the following:

1. A rhodium anode x-ray tube which can be operated at 20 keV with currents up to 100 mA.

2. A 50-ft evacuated tube.

3. A large test chamber at the opposite end of the tube from the x-ray tube. This chamber contains independent crystal and detector holders with calibrated motions and provisions for accepting the prototype satellite polarimeters for testing.

A large number of low-temperature, high-pressure-produced graphite crystals were tested with this facility. The mosaic spread of these crystals was found to be typically 30 to 50% higher than that measured from a small section of each crystal's surface, as shown in Table III.

B. Development of Mosaic Crystals of Tungsten Disulphide

As part of our research program, we subcontracted to the Union Carbide Corporation the development of mosaic tungsten disulphide crystals. On the basis of our theoretical calculations, the mosaic form of this crystalline material was found to have very high integrated reflectivity and therefore to be extremely useful for polarimetry at 1.3 keV and for spectroscopy in the 1 to 2 keV region. X-ray instruments sensitive in this energy region are of particular importance because 1) the typical proposed and existing grazing-incidence x-ray telescopes have relatively poor collection efficiencies for energies much beyond 3 keV; 2) the continuum flux from many of the observed x-ray sources is near maximum in the 1 to 2 keV region; and 3) there are a large number of possible x-ray line emissions in this energy region.

The Union Carbide Corporation has been successful in producing a preliminary form of tungsten disulphide, and their final report is included in Appendix I.

C. Lithium Hydride

Several large samples (2 x 3 x 2 in.) of LiH crystals were purchased from the Lithium Corporation of America. Smaller crystals were cleaved from these samples. The measured integrated intensity of

Table III. Measurement of the Mosaic Spread over Small and Large Areas of the Same Crystal

Sample	Small Area Mosaic Spread[1] (degrees)	Total Crystal Mosaic Spread[2] (degrees)	Increase (degrees)
C2	0.62	0.92	0.30
C4	0.70	0.96	0.26
C7	0.85	1.50	0.65
C14	0.44	0.71	0.27
C25	0.55	0.75	0.20
C27	0.50	0.70	0.20
C28	0.50	0.75	0.25
C29	0.70	0.71	0.04
C26	0.73	0.85	0.12

[1]Three percent of the total area of the crystal was sampled.

[2]Entire crystal area (1 in. x 1 in.) was sampled.

the few samples tested was on the order of 0.8×10^{-3}, at 4.6 keV. The results of one of these measurements are shown in Fig. 1, where three separated Kα (and Kβ) peaks indicate that this crystal consists in fact of three different crystals at angles of 0.8° and 2.7° with respect to the crystal parallel to the surface. This type of behavior is often found in large NaCl-type crystals.

A technique often used for improving the integrated reflectivity of salt-like crystals such as LiH is to bend the crystal. This guarantees that the incident flux must satisfy the Bragg condition at slightly different energies in order to be reflected as it penetrates into the material, thus eliminating secondary extinction. Bending also serves to break up the larger domains. The bending procedure is carried out by slightly heating the crystal in a vacuum and pressing the crystal into shape. An apparatus to achieve this effect was constructed.

In addition to the bending technique, a shock treatment was also prepared in which the crystals were held in place in a mold and cracked with a hammer. The results of these experiments, though inconclusive, proved encouraging. In several cases the integrated reflectivity improved by more than a factor of 10; however, this was on samples that initially tested well below 10^{-4}. The program for the development of the LiH was hampered by the fact that the initial samples from the Lithium Corporation were not uniform in property. We began negotiations with the Harshaw Chemical Company to produce LiH crystals for us but were not able to continue because of lack of funds. This was particularly unfortunate, because of all the crystals, LiH could be used as an

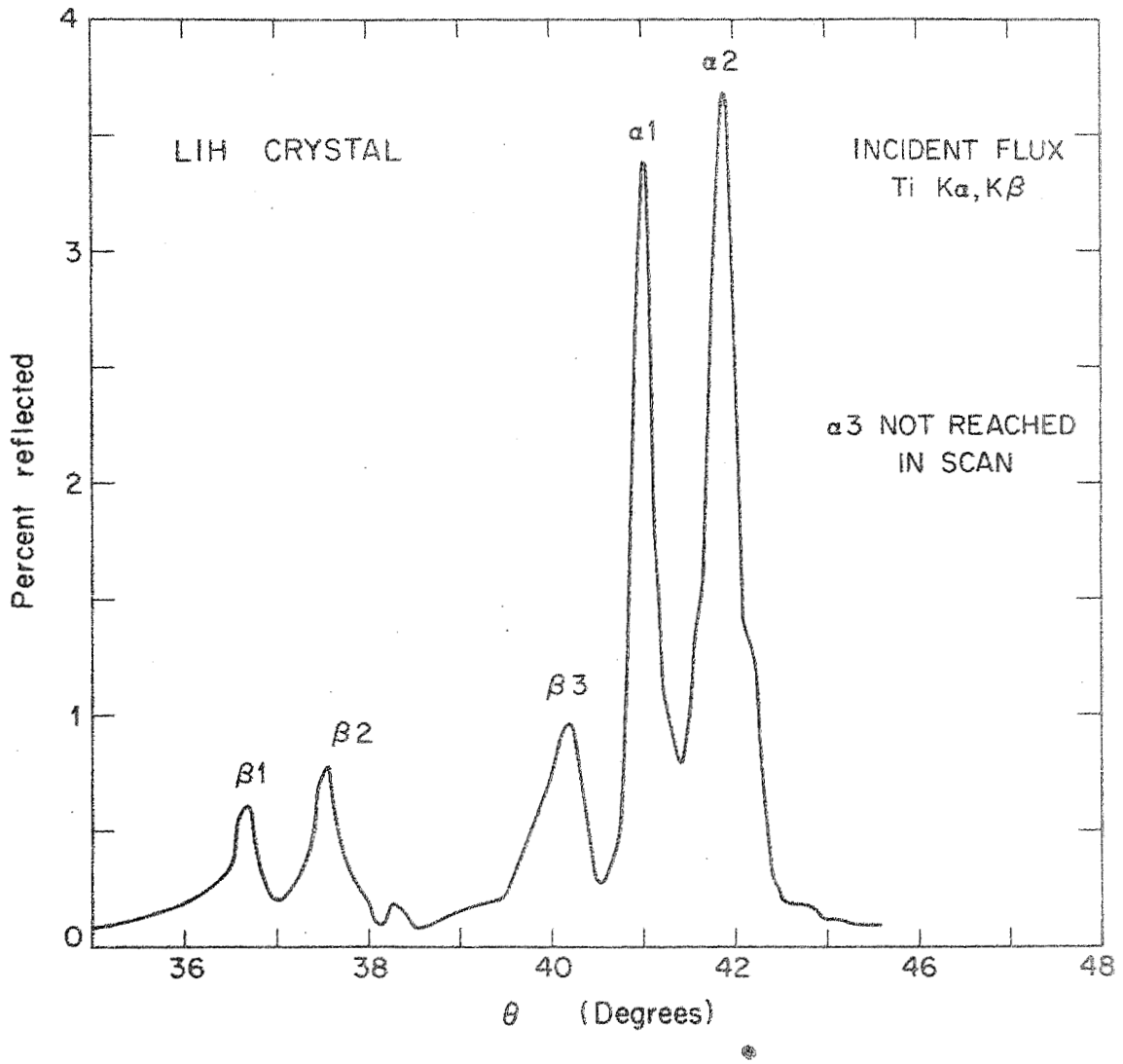

Figure 1. Rocking curve for LiH

extremely efficient polarimeter at 4.3 keV and is one of the best choices of materials for use in an objective crystal spectrometer, as described in Section III.

III. SPECTROSCOPIC INSTRUMENTS EMPLOYING MOSAIC CRYSTALS

Observations of x rays from cosmic sources have been made almost exclusively with large direct-viewing detectors, which for photon energies below 10 keV universally employ proportional counters. The energy resolution thus achieved is at best 15% at 6 keV and becomes broader for lower energies (Culhane et al., 1966). The broad resolution makes the detection of line radiation and absorption edges very difficult, and so far no positive indication of these features has been observed in any cosmic source (Fritz et al., 1969; Holt et al., 1968). Clearly, a large step forward will be made when high-resolution spectra can be obtained by grating or Bragg reflection techniques. These techniques have not been used because the radiation from cosmic sources is extremely weak, and only short observations are possible from sounding rockets.

Even with the long observation times that will become available with satellite-borne equipment, highly efficient instruments will be required to obtain spectra of sources much weaker than the Crab nebula. The most efficient use of Bragg reflection for both spectroscopy and polarization measurements is obtained by exploiting the properties of mosaic crystals with high integrated reflectivity. Examples of such crystals are lithium hydride, graphite, and tungsten disulphide. For part of this program, we have designed a spectrometer to be used in conjunction with a grazing-incidence lens. This device realizes both the high efficiency of a mosaic crystal and the very high resolution possible with Bragg spectroscopy. As this instrument must await the development of large x-ray lenses of high efficiency, we have also considered performing useful survey measurements with simpler spectrometers having no focusing elements.

A. The Objective Crystal Spectrometer

In considering spectrometer design we shall for the moment disregard resolving power and discuss the properties of an analyzing crystal which will maximize efficiency. The criterion used is that the largest possible number of photons should be reflected as a scan is made over a given range of wavelengths.

Suppose a crystal is illuminated with radiation from a cosmic source and is rotated with uniform angular velocity ω to scan from Bragg angle θ_1 to θ_2, and that Bragg reflection of wavelength λ takes place within this range. Let $I(\lambda)d\lambda$ be the power at wavelength λ in the spectral range $d\lambda$ incident on the crystal, and let $R(\theta,\lambda)$ be the coefficient of reflection of x rays of wavelength λ incident at angle θ on the crystal. The total reflected energy in the same spectral range $W(\lambda)d\lambda$ is given by

$$W(\lambda)d\lambda = \int_{\theta_1}^{\theta_2} I(\lambda)d\lambda R(\theta,\lambda)\frac{d\theta}{\omega}$$

$$= \frac{1}{\omega} I(\lambda)d\lambda \cdot \Delta\theta(\lambda) \qquad (1)$$

where

$$\Delta\theta(\lambda) = \int_{\theta_1}^{\theta_2} R(\theta,\lambda)d\theta \qquad (2)$$

The quantity $\Delta\theta$ is the integrated reflectivity. Since the number of photons detected is directly proportional to $\Delta\theta$, the most efficient crystals for Bragg spectroscopy will be those with the highest values of $\Delta\theta$.

The integrated reflectivity is not the same for all single crystals of the same substance, but depends on the degree of perfection of the crystal. It is highest for an ideally imperfect or mosaic crystal, that is, one in which perfect alignment of crystal planes is maintained only over microscopic domains.

A ray entering such a crystal passes through many domains at slightly different Bragg angles before it is absorbed. Crystals normally used for x-ray spectroscopy are chosen to have their crystal planes accurately aligned so that reflection of a given wavelength takes place only over a very narrow angular range, and as a consequence they have poor integrated reflectivity. A perfect crystal has an integrated reflectivity typically 10 or 100 times smaller than an ideally imperfect crystal of the same substance. It would appear at first sight that the requirements of high efficiency and high resolution are incompatible. We shall show below that in fact a stellar spectrometer of very high resolving power can be made with mosaic crystals by making use of a grazing-incidence telescope.

We have first to determine which crystals have the highest values of integrated reflectivity when in an ideally imperfect form. These will then be the most suitable for analysis of the very weak fluxes of x-ray astronomy. The integrated reflectivity of a mosaic crystal is given in the case of unpolarized radiation by the expression derived by Darwin:

$$\Delta\theta = \frac{1 + \cos^2 2\theta}{4 \sin 2\theta} \cdot \frac{N^2 \lambda^3 F^2 r_o^2}{\mu} \qquad (3)$$

Here μ is the absorption coefficient, N is the number of scattering cells/unit volume, F is the crystal structure factor, that is, the effective number of scattering electrons per cell, and r_o is the classical electron radius. A full account of reflection by crystals is given by James (1948). An examination of Eq. (3) shows that $\Delta\theta$ is maximized in crystals with well-defined planes of high electron density, and for scattering atoms whose photoelectric absorption cross section is small compared with the coherent scattering cross section, which is proportional to $F^2 r_o^2$. We have used Eq. (3)

to calculate $\Delta\theta$ for many crystalline materials chosen for these properties; in Table I we have listed the results for radiation incident at 45° on crystals with the highest reflectivity and on some commonly used for x-ray analysis. It will be seen that very high values are obtained for lithium hydride, graphite, and tungsten disulphide.

A crystal will show high integrated reflectivity, close to the theoretical value of Eq. (3), provided that the domains are not too large, as discussed below, and provided that the domains are sufficiently misaligned. A direct measure of the degree of misorientation is the mosaic spread, defined to be the angular full width at half maximum of $R(\theta,\lambda)$ for monochromatic radiation. From Eq. (2) it is clear that the mosaic spread cannot be less than $\Delta\theta$, and in practice it must be a few times greater than $\Delta\theta$. Our samples of graphite show a mosaic spread of 10 $\Delta\theta$ or 1/2°. For lithium hydride the theoretical maximum integrated reflectivity is 1/5°. A crystal with a mosaic spread of about 1° would be expected to yield this high maximum.

Although crystals with high integrated reflectivity must show a broad rocking curve, they can still be used to obtain high resolution spectra. We observe that if such a crystal is illuminated with a parallel monochromatic beam satisfying the Bragg condition, the divergence of the reflected beam is not determined by the mosaic spread, since only those domains which are correctly oriented contribute to the reflection. It is the diffraction of single domains which sets the divergence, and this will generally be much less than the mosaic spread. Thus the wavelength can be accurately determined by measuring the angle between the incident and reflected beams.

This spectroscopic technique is ideally suited to the particular circumstances of astronomical observations. The radiation to be analyzed is

in the form of a well-collimated beam. Most of the brighter x-ray objects are thought to be stars, while even the extended Crab nebula source has an angular diameter of only two arc minutes (Bowyer et al., 1964; Oda et al., 1967). If the direct radiation from a source is incident on a mosaic crystal, a range of wavelengths determined by the mosaic spread is reflected, and a grazing incidence telescope can be used to determine accurately the spectral distribution within this range, as shown in Fig. 2. If there were a sharp emission line in the source, it would appear as a line in the x-ray image detector at the focus of the telescope.

The ideal crystal for this purpose would have high integrated reflectivity and combine this with a very narrow diffraction width for monochromatic radiation. The two properties are not mutually exclusive, and a carefully chosen domain structure can optimize both characteristics, as we now show. The angular distribution of reflected radiation depends on the details of the crystalline structure. When illumination is by a parallel beam of monochromatic x rays, the diffraction observed will be determined essentially by the size of the regions which are actually reflecting. For a mosaic structure in which the domains are very small, the diffraction width varies inversely with the domain size. The lowest possible width is achieved when reflection is nearly complete as radiation passes through a single correctly oriented domain. The crystal should have domains just large enough for this to occur, but no larger. Any further increase in size will not increase resolution, but will attenuate the beam by photoelectric absorption and incoherent scattering, and the maximum integrated reflectivity will not be achieved.

The natural diffraction width for a large domain is given by the expression

$$\Delta\theta_N = N\lambda^2 F r_o \frac{1 + |\cos 2\theta|}{\pi \sin 2\theta} \qquad (4)$$

due to Darwin (1914) and Prins (1930). As a measure of the ideal domain size,

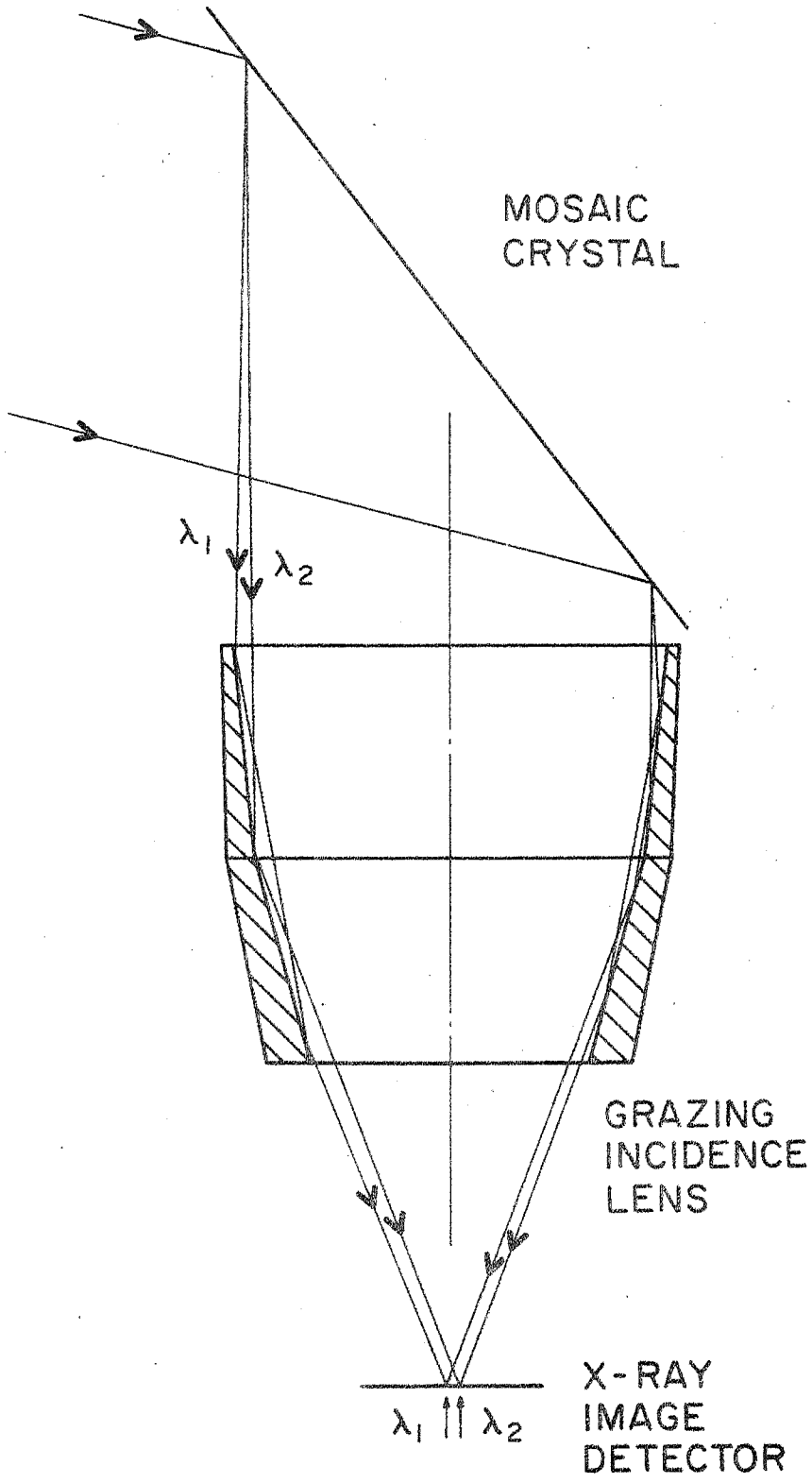

Fig. 2. Bragg spectrometer making use of a grazing-incidence lens.

we take the distance d, measured along the ray, in which the transmitted intensity of x rays satisfying the Bragg condition is reduced by a factor 1/e. The reflected beam in this case will have a diffraction width nearly as small as the limiting value of Eq. (4). Following the treatment of James (1948), pp. 52-63, we obtain

$$d = \frac{2\lambda\ (1+|\cos\ 2\theta|)}{\pi^2 \sin 2\theta \Delta\theta_N} \tag{5}$$

The quantities $\Delta\theta_N$ and d obtained from Eqs. (4) and (5) for graphite and lithium hydride are given in Table IV, together with the corresponding resolving power obtained from the relation

$$R = \frac{\lambda}{d\lambda} = \frac{\tan\ \theta}{\Delta\theta_N} \tag{6}$$

For photon energies above 3.5 keV, lithium hydride would be an ideal analyzing crystal. The extremely high integrated reflectivity already pointed out is combined with a very narrow natural diffraction width. We see that at 4 keV the diffraction width is 2 arc sec, which would yield a resolving power of 100,000. The domain thickness should be about 5 microns, measured perpendicular to the surface, for then the penetration depth d would be close to optimum for a range of wavelengths. For photon energies between 2 and 4 keV, graphite would be a good crystal, the theoretical resolving power being greater than 5000 over the range 2-5 keV. The optimum domain thickness required for graphite is about 10^{-4} cm. Samples with high integrated reflectivity have been measured in this laboratory with chlorine K_α radiation and are found to have a diffraction width below the instrumental resolution of about 2 arc min. Such material would thus yield a resolving power of at least 2000, and it seems likely that samples with the optimum domain structure could be prepared by existing techniques.

TABLE IV

Diffraction from Single Domains

Crystal	Photon Energy (keV)	Bragg Angle θ (degrees)	Diffraction Width $\Delta\theta_N$ (arc seconds)	Ideal Domain Size d (microns)	Resolving power
Graphite	2.0	67.8	86	0.7	6000
	3.0	38.1	7	1.1	8000
	4.0	25.6	17	1.5	6400
Lithium hydride	3.5	60.1	5	5.1	70,000
	4.5	42.4	2	6.6	98,000
	5.5	33.5	2	8.0	86,000

It appears that grazing incidence lenses could be made with sufficient resolution, field of view, and energy response to match the properties of the crystals just discussed. As an example of the geometrical imaging properties which can be achieved, we consider the A.T.M. parabola-hyperbola lens described by Magnus and Underwood (1969), which has a maximum grazing angle of 0.92°. With optimum geometry, the focal spot is no bigger than 10 sec of arc (half intensity width) over the whole field of view of 2/3°. For most of the field the spot size is well under 10 arc sec. Such a field of view is sufficient to bring to a focus most of the reflected energy from a crystal with a mosaic spread of 1/3°. A gold-coated lens with 0.9° grazing angle would have a high-energy cut off at about 4 keV, the reflection efficiency dropping rapidly above this energy. To obtain effective response at 6 keV, grazing angles of about 0.6° would be required, and there would be a corresponding reduction in the field of view. Thus we see that a lens could bring to a focus with sufficiently high resolution the radiation in the 2-4 keV range reflected from graphite crystals. In order to make the best use of lithium-hydride reflection in the 4-6 keV range, it will be necessary to prepare material with as small a mosaic spread as possible, so that the reflected radiation falls within the reduced field of view of a high-energy lens. An interesting possibility is that the large domain structure could be prepared artificially by cleaving sheets of about 10^{-3} cm in thickness and stacking them one above the other at slightly different angles. In this way it is theoretically possible to obtain close to the maximum integrated reflectivity of 1/5° with a mosaic spread of about the same size. Alternatively, it may be possible to obtain the same result by using a crystal made from slightly curved sections. The most serious practical problem with x-ray lenses for any work with cosmic sources is the difficulty of obtaining a

large collecting area. In principle, many surfaces can be nested to give higher areas, but these techniques are not yet far developed. The realization of the proposed instrument must await the development of large x-ray lenses to be carried on satellites with good pointing accuracy.

We wish to emphasize that mosaic crystals can be used to obtain very high-resolution spectra which conventional well-ordered crystals could achieve only with a great loss in sensitivity. Let us suppose that a conventional spectrometer is made with a resolution of 5,000 at a Bragg angle of 45°. By a conventional spectrometer we mean one in which the Bragg angle is determined by the setting of the crystal rather than by the measured angle between the incident and reflected beams. A highly aligned crystal with a rocking curve of about 2×10^{-4} radians in width must be used. The value of $\Delta\theta$ given by Eq. (2) must thus be less than 2×10^{-4}. If now a range of wavelengths is scanned, perhaps to obtain a line profile or to search for a weak line, then the total number of photons detected is proportional to $\Delta\theta$. A spectrometer with a mosaic crystal of integrated reflectivity equal to 10^{-3}, having the same area and scanning the same range for the same time, will thus detect at least five times as many photons, and the wavelength of each one can be resolved to 1 part in 5000 provided the telescope has a modest resolution of 40 arc sec.

The combined use of the mosaic crystal and the focusing optics of an x-ray telescope as described above leads to a spectrometer of the highest efficiency and resolution. The fact that a relatively large fraction of the spectrum is observed at a single setting of such an instrument is an important advantage. This feature not only minimizes the time necessary to scan the spatial region covered by the spectrometer, but also allows for the simultaneous observation of the intercombination and forbidden lines in the helium I-like spectrum of several elements, such as those seen in solar x-ray spectra. The relative intensities of these two lines are of paramount importance as they

provide a direct measurement of the electron density of the emitting region.

We have incorporated the results of our study of the objective crystal spectrometer in a proposal with American Science and Engineering, Goddard Space Flight Center, and the Massachusetts Institute of Technology for the third HEAO mission.* This spectrometer would employ two crystalline materials, graphite and tungsten disulphide, each with a mosaic spread of 1/4°; the energy range from 1 to 4 keV would be covered in 320 settings (in order to scan the Bragg angles from 30° to 70° in 1/4° steps for each crystal). The effective area of the telescope to be used with these crystals is shown in Fig. 3. The wavelength ranges that each of the crystals would cover are also shown in the figure. As can be seen, these crystals were chosen not only for their high reflection efficiency, but also for their compatibility with the energy response of the telescope.

The principal range of energies scanned by each crystal corresponds to Bragg angles from 30° to 70°. These limiting angles were chosen in order to cover all the known spectroscopic features of interest in the energy range from 1 to 4 keV, without unduly increasing the size of the crystal panels necessary to guarantee full illumination of the lens. (A full description of the lens is contained in the Loxt Proposal.* Energy as a function of Bragg angle for the two materials is listed in Table V.

Table V

Graphite (2D = 6.70 A)		WS_2 (2D = 12.5 A)	
Bragg Angle (Degrees)	Energy (keV)	Bragg Angle (Degrees)	Energy (keV)
30	3.71	30	1.98
40	2.89	40	1.54
50	2.42	50	1.30
60	2.14	60	1.15
70	1.97	70	1.06

*See Loxt Technical Proposal - 2410-1, prepared for NASA, 27 May 1970.

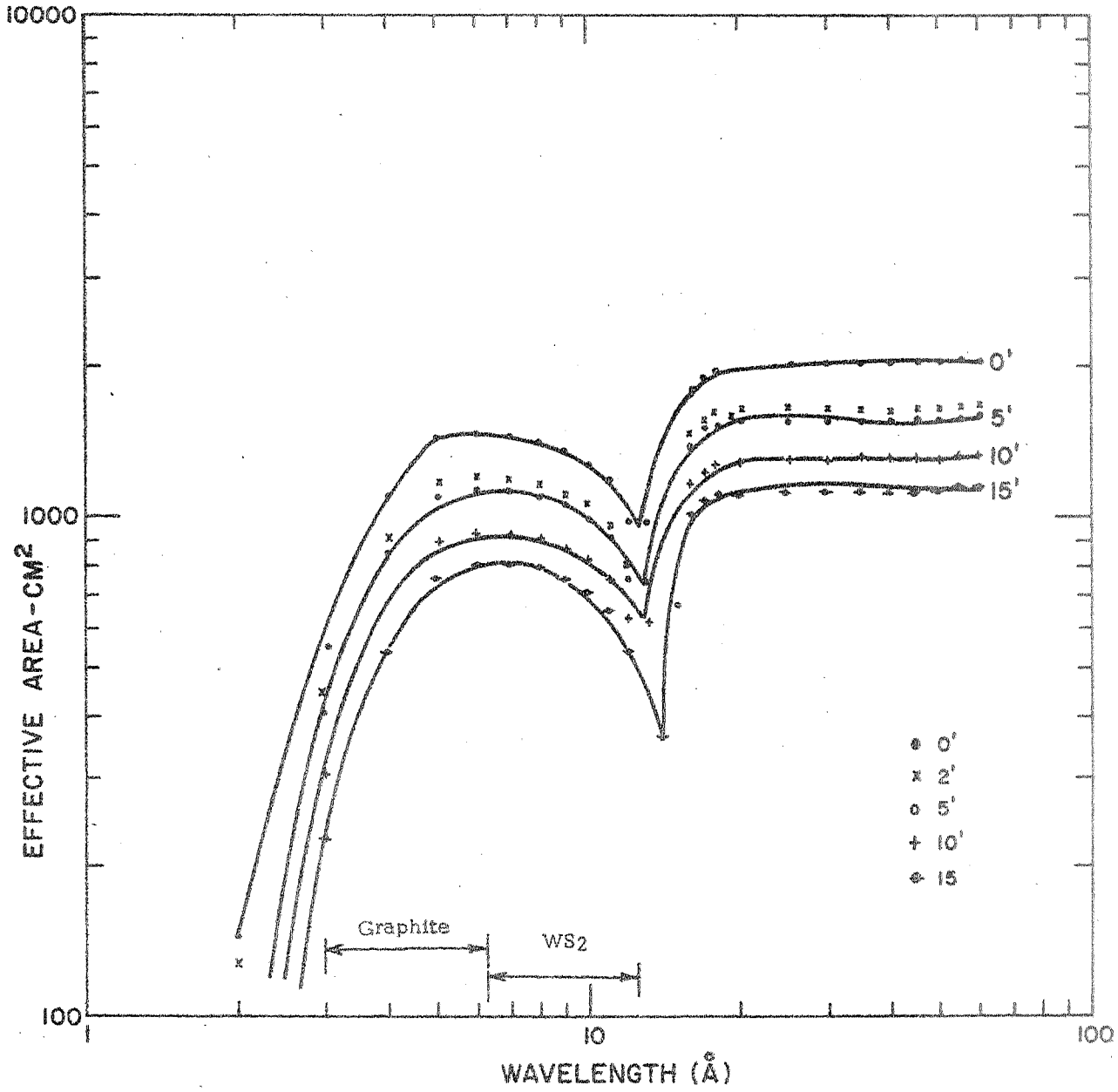

Figure 3. Effective Area of High-Resolution Telescope and Wavelength Acceptance Intervals of Graphite and WS_2

The graphite crystal would also be used to scan down to 27° in order to search for the Lyman α emission of hydrogenic calcium at 4.07 keV. Similarly, the tungsten disulphide crystal will be scanned to 77° in order to search for L_α of Neon X. A list of the energies of the Lyman α emission from hydrogenic ions covered by the energy response of the spectrometer is given in Table VI. It should be noted that all of the x-ray emission lines listed in Table VI have been observed in solar spectra.

Table VI

Lyman α Spectra Within the Energy Response of the Objective Crystal Spectrometer

Element	Z	Crystal	Energy (keV)	Fine-Structure Separation (eV)	Bragg Angle (degrees)
Neon	10	WS_2	1.02	0.4	76.5
Magnesium	12	WS_2	1.47	1.0	42.4
Silicon	14	C	2.00	1.8	67.7
Sulphur	16	C	2.61	3.0	45.1
Argon	18	C	3.30	4.0	34.1
Calcium	20	C	4.08	7.3	27.0

Other features of interest within the energy response of the spectrometer are the helium I-like spectra of certain ions listed in Table VII and the absorption edges caused by certain elements listed in Table VIII.

Table VII

Helium I Spectra Within the Energy Response
of the Objective Crystal Spectrometer

Element	Resonance Line $(1^1S_0 - 2^1P_1)$ (keV)	Intercombination Line $(1^1S_0 - 2^3P_1)$ (keV)	Forbidden Line $(1^1S_0 - 2^3S_1)$ (keV)
Magnesium XI			
Silicon XIII	1.867	1.856	1.840
Sulphur XV	2.458	2.446	2.429
Argon XVII	3.139	3.124	3.103
Calcium XIX	3.906	3.890	3.866

Table VIII

Absorption Edges Within the Energy Response
of the Objective Crystal Spectrometer

Element	K Absorption Edge (keV)
Magnesium	1.30
Silicon	1.84
Sulphur	2.47
Chlorine	2.82
Argon	3.20
Potassium	3.61
Calcium	4.04

The width of the spectrum observed at a particular setting of the spectrometer is shown as a function of energy in Fig. 4. We note from Fig. 4 and Table VII that the entire triplet of either Calcium XIX or Argon XVII will be observable at a single setting of the instrument, and further that the intercombination and forbidden lines of all the ions listed in the table are simultaneously observable when the instrument is adjusted to reflect the appropriate energies.

We estimate the contributions to typical x-ray emission linewidths from sources such as Scorpio X-1 ($T = 5 \times 10^7$ °K) in Table IX. The dominant contribution to the minimum linewidths at these temperatures and energies arises from ion Doppler broadening and is on the order of a few electron volts over the energy range covered by the spectrometer. The resolving power of any stellar x-ray spectrometer should then be on the order of one to two thousand to resolve these lines adequately and to study their shapes.

Table IX

Estimate of Linewidth at $T = 5 \times 10^7$ °K

Ion	Photon Energy (keV)	Ion Doppler Width (eV)	Natural Width (eV)	Auger Width (eV)
Si XIV	2.00	1.15	~ 0.02	~ 0.23
S XVI	2.61	1.40	~ 0.03	~ 0.35

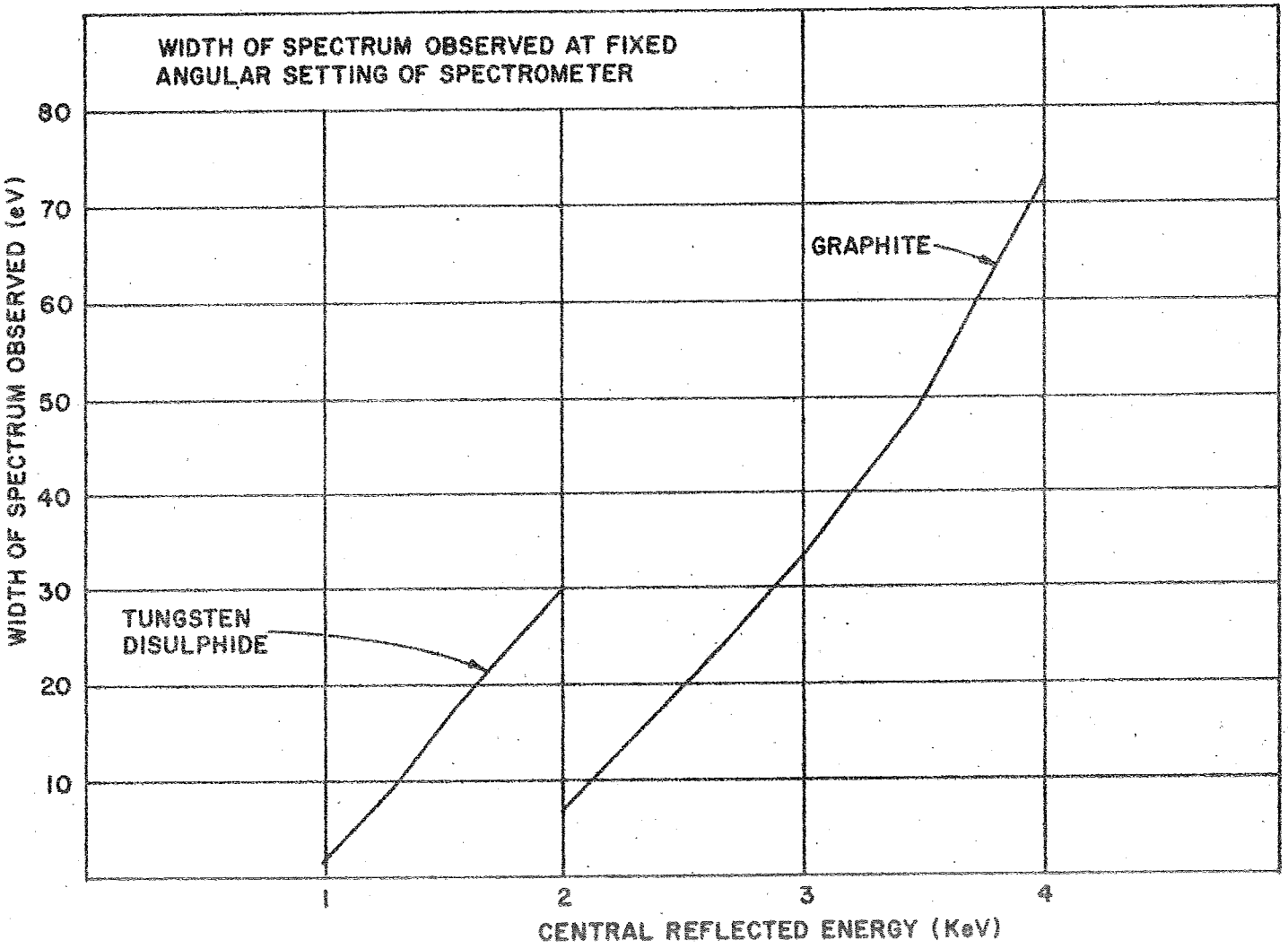

Figure 4. Spectral acceptance at a single crystal angle as a function of central ray energy

Table X

Optimum Domain Size and Diffraction Limited Widths
for Monochromatic X-Rays

Graphite			Tungsten Disulphide		
Energy (keV)	Domain Size (cm x 10^5)	Diffraction Limited Width (eV)	Energy (keV)	Domain Size (cm x 10^5)	Diffraction Limited Width (eV)
2.0	9.5	0.26	~ 1.0	1.6	1.5
2.5	11.9	0.21	1.5	2.1	1.5
3.0	14.3	0.29	2.0	2.8	2.7
3.5	16.7	0.39			
4.0	19.0	0.48			

Theoretical integrated intensities have been observed for a large fraction of the graphite crystals that Columbia University received from Union Carbide Corporation. Direct measurements have been made in the Columbia Astrophysics Laboratory with chlorine K radiation (2.6 keV), and the samples were found to have a diffraction width below the instrumental resolution of about 2 arc min. This result is consistent with the theoretically predicted width of about 20 arc sec at this energy.

The 30 arc-sec resolution of the proposed telescope is greater than the diffraction-limited resolution of the spectrometer at all except the lowest energies scanned. In Table XI we show the resulting instrumental resolution when both the 30 arc-sec resolution of the telescope and the geometrical off-axis effects are taken into account. The instrumental

widths and resolving powers in Table XI are averages over the entire ± 1/2° field of view of the telescope and therefore represent upper and lower limits, respectively.

Table XI

Instrumental Resolution

Energy (keV)	Average* Instrumental Resolution (eV)	Resolving Power	Material
1.25	1.38	910	WS_2
1.5	1.87	800	WS_2
1.75	3.02	580	WS_2
2.0	4.34	460	WS_2
2.0	0.37	5465	C
2.5	0.68	3665	C
3.0	1.14	2635	C
3.5	1.71	2050	C
4.0	2.63	1520	C

* Averages over the field of view of the telescope.

For most of the energy range covered by the graphite crystals, the average resolution corresponds to better than 2 arc min over the field of view of the telescope. Thus there are typically thirty resolution elements available for simultaneous observation at a single setting of the spectrometer in the spectral region from 4 to slightly above 2 keV. Comparing the resolution in Table XI with the emission linewidths estimated

in Table IX, we see that the resolving power of this spectrometer is ideal for high-resolution extra solar spectroscopy.

Absorption coefficients are from the tables of Leroux (1963), except that of lithium, which is from Henke et al. (1967). The atomic structure factors are from Hanson et al. (1964). The crystal structure factors were calculated from the atomic locations in Wyckoff (1963).

When the parallel radiation (continuum plus lines) from an x-ray source is incident on the spectrometer, the reflected continuum (noise) contribution is uniformly distributed over all the resolution in the field of view, whereas the line contribution (signal) will be contained in a very few resolution elements resulting in favorable signal-to-noise ratios. For example, the continuum contribution from Sco X-1 at 2.6 keV will give rise to approximately 0.5 ct/sec/resolution element in each of 60 resolution elements, whereas the sulphur line at the same energy will be contained within four 0.75-eV resolution elements at an average rate of approximately 1 ct/sec/resolution element, if the line intensity is only 0.1% of the continuum intensity between 2 and 10 keV. We have estimated the sensitivity of the spectrometer for the detection of two of the possible emission lines from Scorpio X-1 in Table XII, where we have reduced the predicted line intensity by a factor of 10. In these calculations we have included detector efficiency and the average response of the instrument as indicated in Table XI, ignoring the fact that at the center of the field of view the resolution is higher by a factor of two.

The mosaic crystal, with its high integrated reflectivity, guarantees that the largest possible fraction of the incident flux

Table XII

Sensitivity to X-Ray Line Emission from Sco X-1

Element	Energy	I_C	Area	I_L	F
Si^{+13}	2.00	39.6	1250	0.044	108
S^{+15}	2.61	34.5	1250	0.050	86

Legend:

I_C (keV/keV-cm^2-sec): Continuum flux

I_L (photons/cm^2-sec): Incident line radiation - 10% of Tucker's estimate

F (dimensionless): The number of standard deviations above the continuum such a line would be after 1000 sec of integration

(continuum plus lines) is reflected at a single setting of the crystal, thus making such crystals ideal for an objective spectrometer. In this application, the reflected flux is distributed among a number of resolution elements whose width is determined by the domain size, and may be resolved by the focusing properties of the telescope. The number of spectral resolution elements is determined in turn by the ratio of the mosaic spread to the width of reflection from a single domain. The actual efficiency for reflection within a resolution element may be somewhat less than if a perfect crystal were employed, but the number of resolution elements received simultaneously is always larger, on the order of 30 or more. (There is, of course, only one resolution element at any one setting of a perfect crystal.) The features of combining high resolution, reasonably high efficiency per resolution element, and an extremely large number of resolution elements make an objective crystal spectrometer of this type ideal for use as a scanning spectrometer and for the detailed study of the line emission from thermal x-ray sources.

B. The Conventional Scanning Crystal Spectrometer

In order to test and develop most of the concepts described previously, a spectrometer consisting of two large (17 in. x 9 in.) reflecting graphite crystal panels (see Fig. 5) was constructed for use with a sounding rocket in a search for the Lyman-α emission of ionized sulphur from Sco X-1. The panels were mounted on two doors which were opened when the rocket was above the atmosphere. The scan over a range of Bragg angles was achieved by changing the attitude of the rocket with the doors fully opened to 45°. Those x rays satisfying the Bragg condition

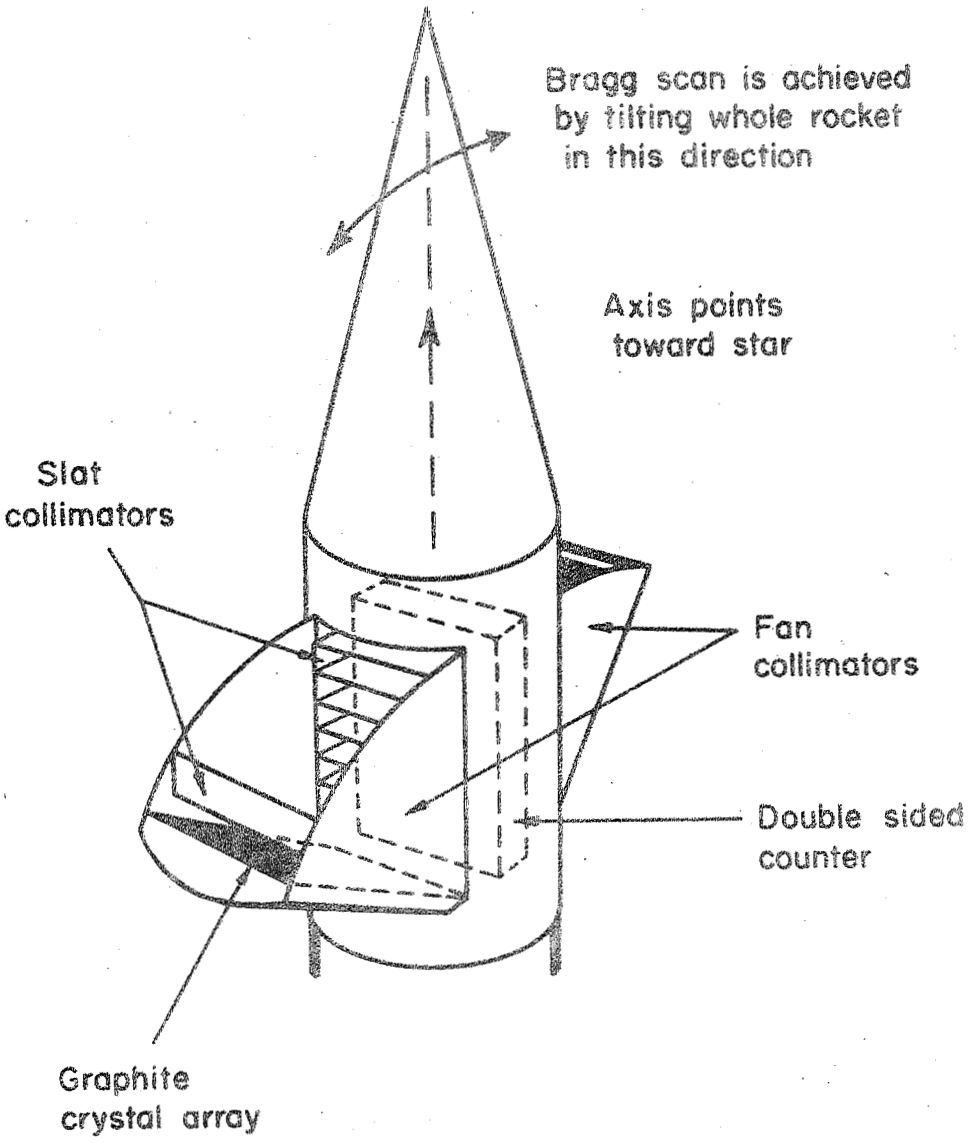

Fig. 5. The spectrometer.

were reflected into a central bank of proportional counters, and the detected pulses were telemetered to the ground.

The graphite crystal panels were constructed from 150 crystals, each one-inch square. The crystals were aligned in the large panels, using both optical and x-ray techniques. Each crystal, mounted on its own three-legged stand, was placed on a glass flat in a beam of parallel light incident at about 45°. The reflected light was focused by a lens onto a screen. The legs of the crystal mount were then carefully sanded down until the reflection from the crystal (a blurred spot on the screen caused by the mosaic property) was centered on the reflection from the glass flat (focused to a point), thus insuring that the crystal face was parallel to the glass flat. The characteristic width of the rocking curve (FWHM) for an individual one-inch-square crystal fully illuminated by a uniform beam of Rh L_α radiation (2.7 keV), collimated to 0.12° was found to be 0.7° with a peak reflectivity of approximately 6.5%. It was found that, for more than 93% of the first 119 crystals mounted and tested, the rocking-curve peaks fell within a range of 10 arc minutes. Optical alignment methods were used exclusively after this correlation had been established. The completed panels were extensively tested in the CAL 150-foot vacuum facility, using a uniform x-ray beam collimated to 0.12° at two different energies. The measured characteristics are shown in Table XIII.

Figure 6 shows a Bragg scan with Panel I of the K_α and K_β lines produced with a chlorine fluorescence source. This instrument, flown successfully aboard an Aerobee-170 rocket in April 1970 in conjunction with the Kitt Peak National Observatory, scanned the spectral range from 2.4 to 2.9 keV of the x-ray emission from Sco X-1. The spectrum obtained showed

Table XIII

Reflection Properties of the Spectrometer Panels

	Panel I	Panel II
FWHM	0.65° ± 0.05°	0.75° ± 0.05
Resolution	29.9 eV	34.5 eV
Resolving Power	87.7	75.8
Peak Reflectivity	6.94% ± 0.18%	5.78% ± 0.15%
Size	9 x 17 in.	9 x 17 in.

no features within this energy range. From the known response of the instrument, this result set an upper limit for the sulphur line emission of about 10^{-3} of the power in the 2-8 Å continuum, an order of magnitude lower than the best proportional-counter experiments of Holt et al. (1970) for the iron line emission. The sensitivity of the instrument may be judged from the upper limit (3σ) of 0.08 photons/cm^2/sec which we placed on the line emission as compared with a flux predicted by Tucker (1967) of 0.55 photons/cm^2/sec for the S^{+15} line intensity from an isothermal, optically thin plasma at 5×10^7 °K.

Detailed descriptions of the experimental hardware and the scientific interpretation of the results of this flight are included in Appendixes II and III. In the context of this report, the most important result of this experiment is that we have shown that large crystal panels can be constructed from smaller sections of mosaic crystals without any loss of sensitivity, thus making possible the construction of the large-area panels necessary for the HEAO.

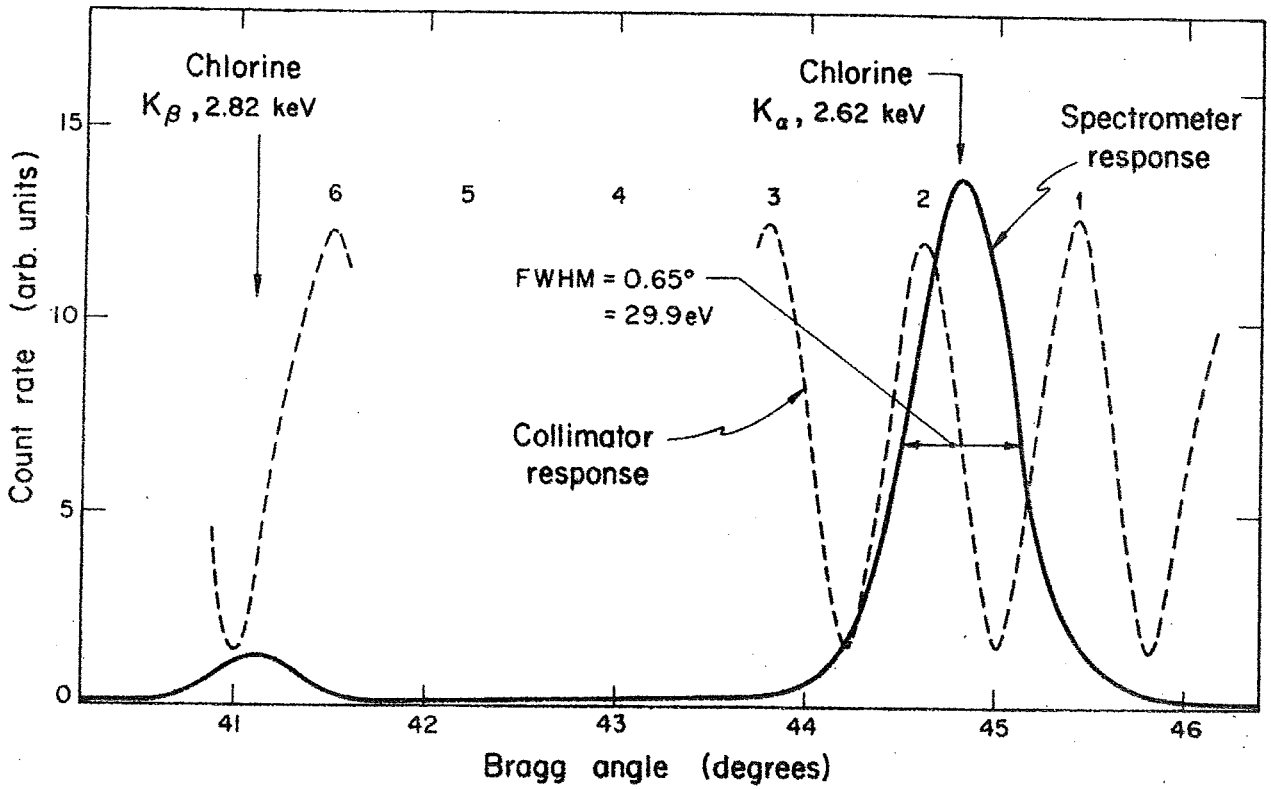

Fig. 6. Laboratory measurement of the reflection from one panel showing peaks due to the K_α and K_β lines of chlorine. The broken line shows the response of the modulation collimator detector permanently fixed to the crystal panel.

IV. FOCAL PLANE CRYSTAL POLARIMETERS

A. Introduction

Even with the long observation times available with satellite-borne equipment, highly efficient instruments will be required to obtain polarization information from sources much weaker than the Crab nebula. Polarization measurements of celestrial sources have so far employed devices based on incoherent scattering of x rays in low-Z material (Angel et al., 1969). Such polarimeters are severely limited for operation in conjunction with grazing-incidence telescopes because of the relatively low high-energy cutoffs ($\simeq$ 4 keV) of these lenses. Except in the case of solid hydrogen, which presents difficult engineering problems, the efficiency of such polarimeters is severely limited because of the high photoelectric absorption cross sections at these low energies. Bragg reflection at 45° incidence offers an attractive way of detecting polarization at the low energies for which a grazing-incidence x-ray lens is sensitive. The polarimeters which we have designed as part of this study make the most efficient use of Bragg reflection for polarization measurements by exploiting the properties of mosaic crystals with high integrated reflectivity.

The crystal polarimeters make use of the fact that when x rays are Bragg-reflected through 90°, only the polarization component of the incident flux that is normal to the incident and reflected rays contributes to the reflected power. The component parallel to the reflected ray is absorbed. The mosaic form of a crystal is used in order to guarantee that the maximum possible power is reflected. As before,

the choice of lithium hydride, graphite, and tungsten disulphide for use as the most efficient polarimeter crystals is a primary result of this study.

The use of crystal polarimeters in conjunction with a grazing-incidence x-ray telescope is attractive not only from a scientific viewpoint but also in terms of their cost and construction. The instruments that we have designed are not only highly efficient but are also simple in design and small in size.

B. Design of Polarimeters at the Focus of the High Efficiency Telescope

The dimensions of any crystal used as a polarimeter at the focus of a grazing-incidence telescope are determined by the size of the x-ray image and the absorption length in the material for the particular energy studied. The length and width of the crystal must be large enough so that the projected face of the crystal encompasses all of the incident flux. For a telescope of 26-ft focal length, such as the high-efficiency telescope described in our HEAO-C proposal, the image size should always be contained within 1/2 in. ($\simeq$ 5 min). The depth of the crystal along the optical axis has to be on the order of a few absorption lengths at the appropriate wavelength in order to maximize the probability of reflection.

The small image size makes practical a design for a graphite polarimeter with improved efficiency over that achieved by a thick piece of the same material. In this type of construction, the crystal is divided into several thin pieces, much less than an absorption length thick, and the pieces are separated as shown in Fig. 7. This procedure

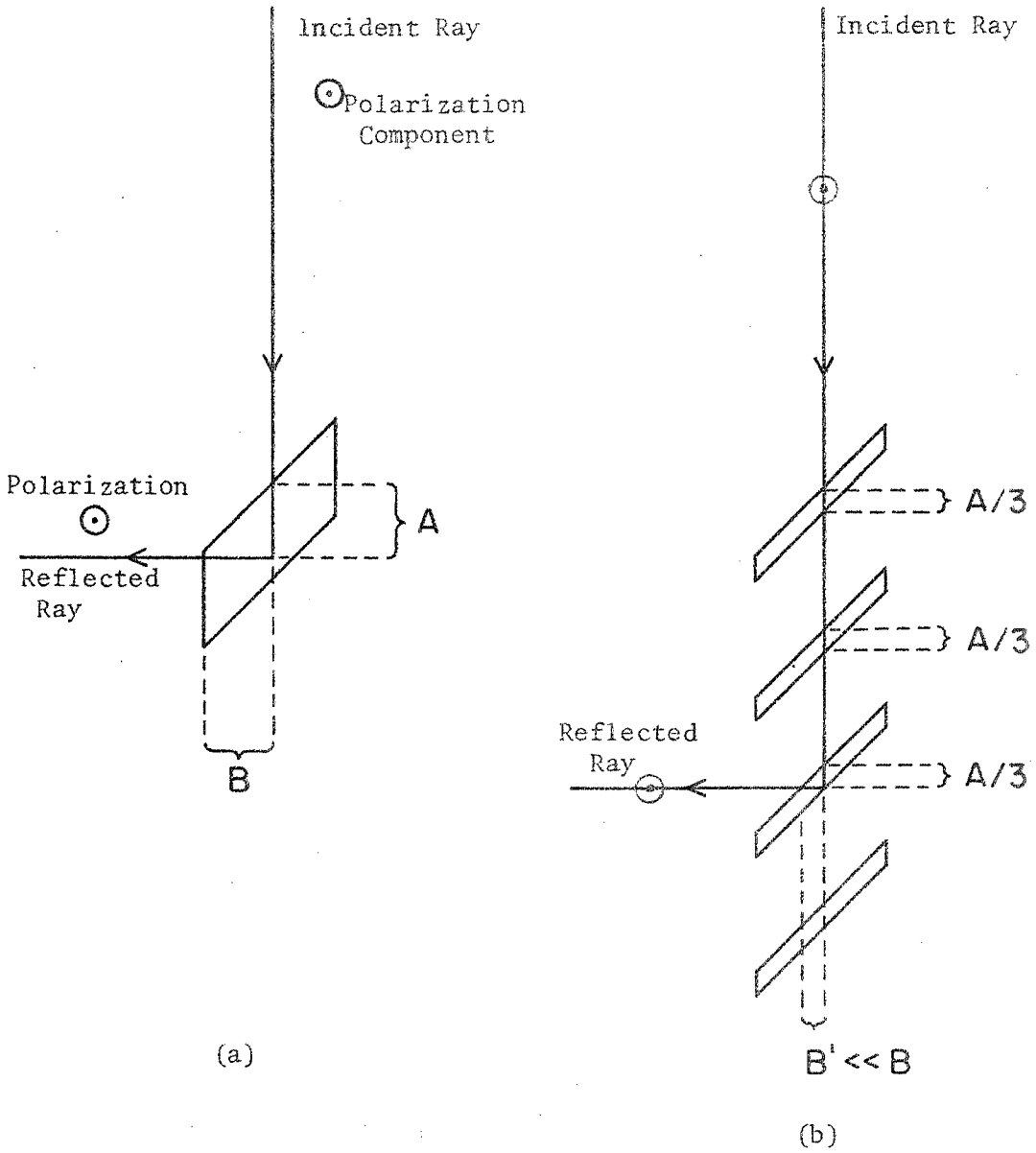

FIG. 7. Graphite polarimeter concept

reduces the probability of absorption in the material after Bragg reflection tales place and, in principle, can be used to increase the integrated intensity of the reflection by a factor of two. A prototype of such a polarimeter has been constructed and is shown in Fig. 8; its performance characteristics are shown in Fig. 9. In this particular version, theoretical integrated intensity was achieved with three thin strips of crystal, with over 35% of the incident flux still available for reflection after passing through the polarimeter.

An artist's sketch of a flight design of a graphite polarimeter is shown in Fig. 10. In this version, the reflected flux is detected in two mutually opposite detectors in order to detect and eliminate systematic effects arising from off-axis x rays.

An increase in the integrated intensity reflected from a crystal can also be achieved by cleaving the material so that the reflecting planes are at an angle with respect to the surface of the material as shown in Fig. 11. This technique will increase the integrated intensity as long as the dimension of the crystal along the reflected ray is less than an absorption length. If this dimension is greater than an absorption length, then the probability of absorption after reflection occurs is increased and the reflected power is reduced.

The absorption length in graphite at 2.6 keV (the energy at which the 90° reflection occurs) is about 0.001 in. If the technique described above were used, the width of the crystal would be much smaller than the expected image sizes. However, for a material such as lithium hydride, the absorption coefficient is about 0.5 $in.^{-1}$, which corresponds to about 5 min at 26 ft, and thus the second method is feasible.

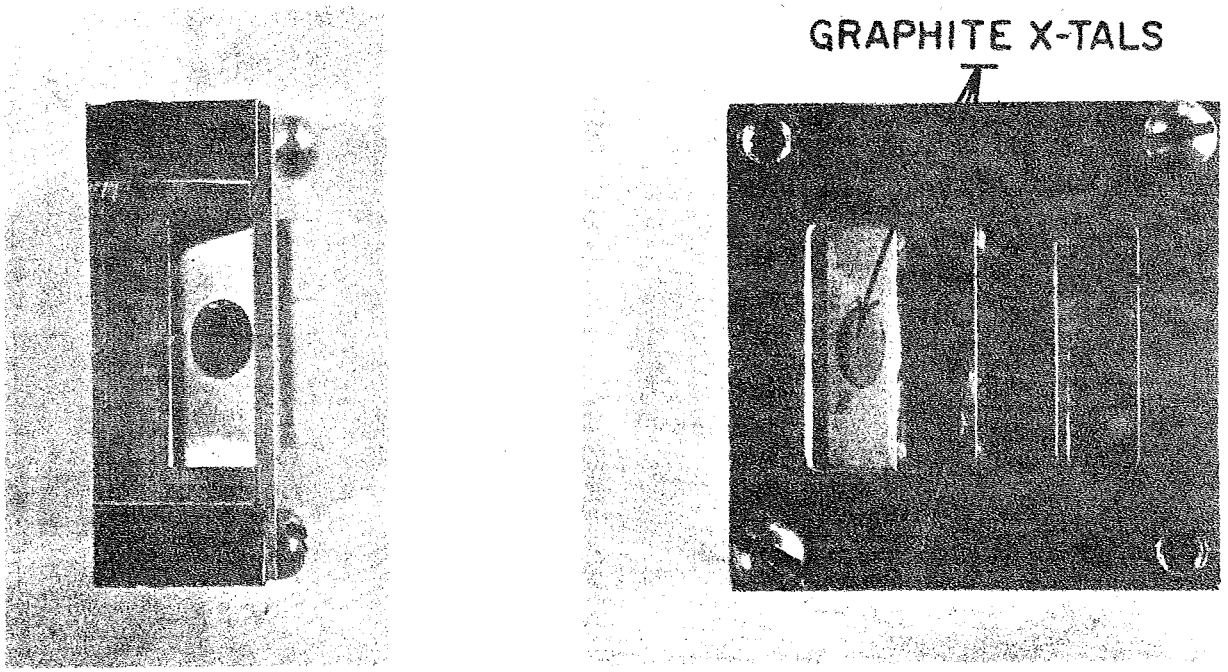

Figure 8. Prototype mosaic crystal polarimeters.

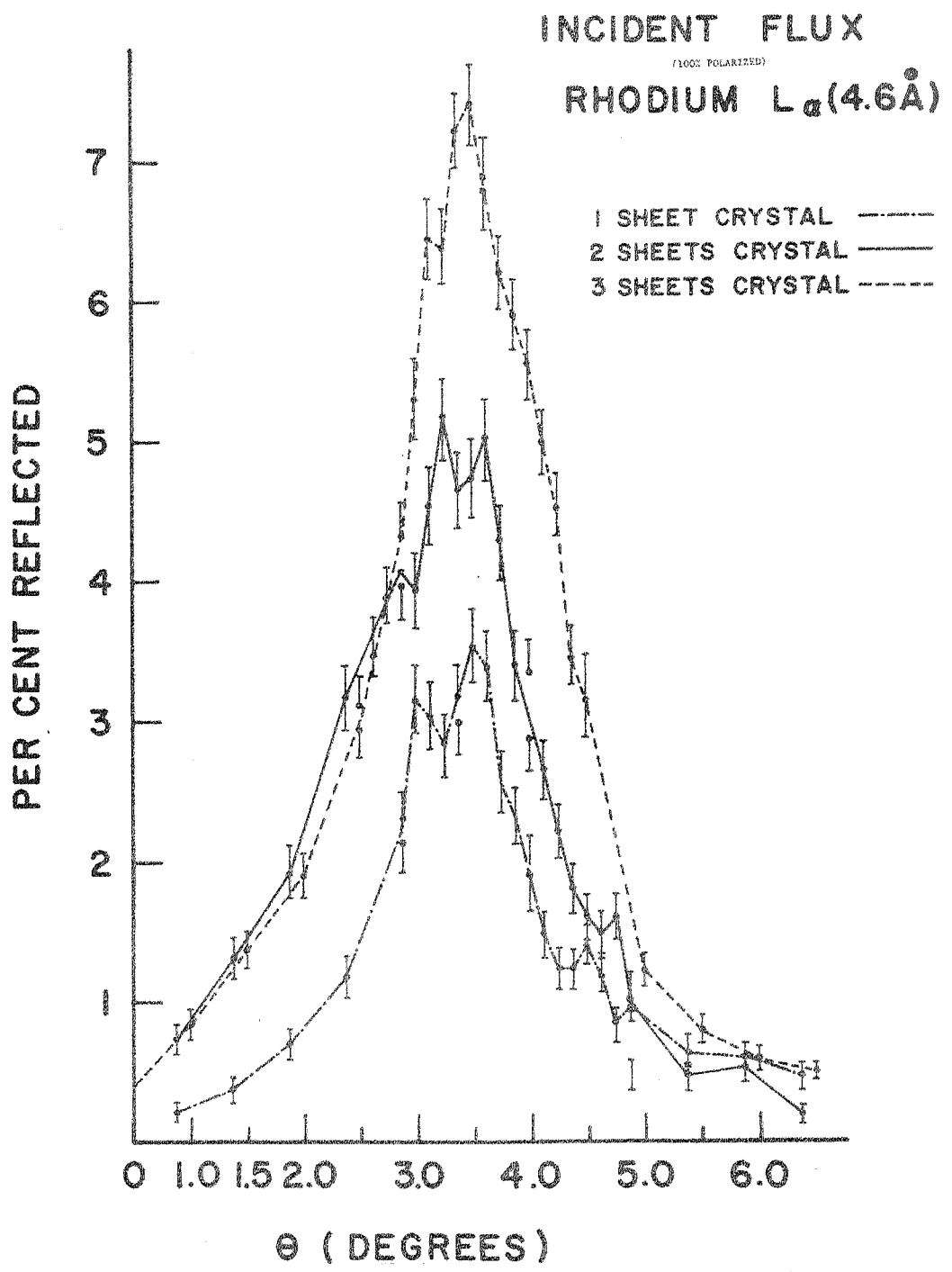

Fig. 9. Experimental reflectivity curves of prototype mosaic crystal polarimeters.

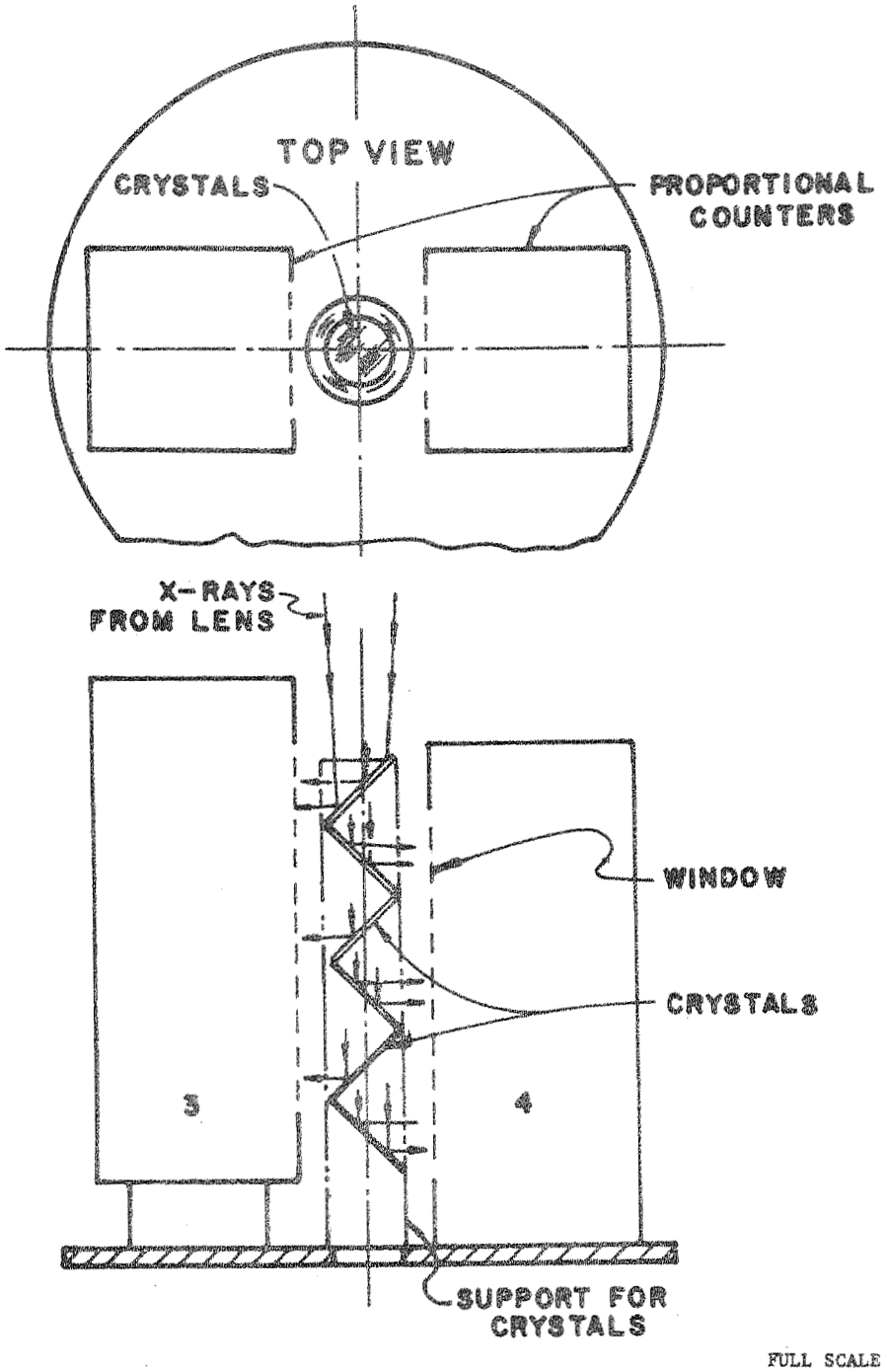

Figure 10. Detector geometry for mosaic crystal polarimeter.

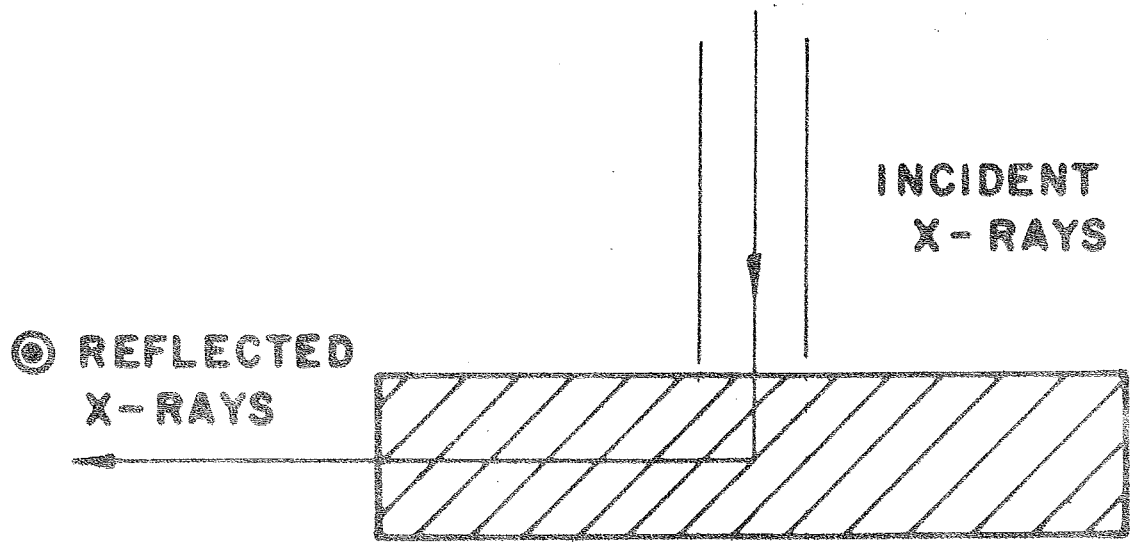

FIG.5

Figure 11. Mosaic crystal cleaved at an angle to increase effective reflectivity by minimizing the length of the exit ray in the crystal. This technique is only applicable if the distance the reflected ray traverses in the crystal is less than an absorption length.

One can take advantage of the symmetric cubic structure of LiH to obtain a further increase in the efficiency of a polarimeter using this material. In LiH there are two orthogonal sets of planes with the same d spacing available for reflection. When the principal (002) planes are oriented at 45° to the front surface of the crystal, coherently scattered radiation appears at both sides of the crystal, as shown in Fig. 12. For a LiH polarimeter, the features of cubic symmetry and large absorption length result in an overall efficiency, which is a factor of four greater than that achieved by a single thick crystal of the same material. Tungsten disulphide is similar to graphite in crystal structure. The material is characterized by dense, widely separated planes of atoms. As this material has neither the cubic symmetry of the LiH nor a small absorption coefficient, the separation technique for increasing efficiency could be utilized.

C. Sensitivity of the Polarimeters

The energies and wavelengths at which the 90° reflection occurs from the three polarimeter crystals are shown in Table XIV. The effective area of the telescope as a function of wavelength is shown in Fig. 13. The wavelengths at which the crystals are sensitive are also marked in the figure.

Table XIV. Energy and Wavelength for 90° Reflection from Polarimeter Crystals

Crystal Material	Energy (keV)	Wavelength (A)
WS_2	1.41	8.79
C	2.62	4.73
LiH	4.30	2.88

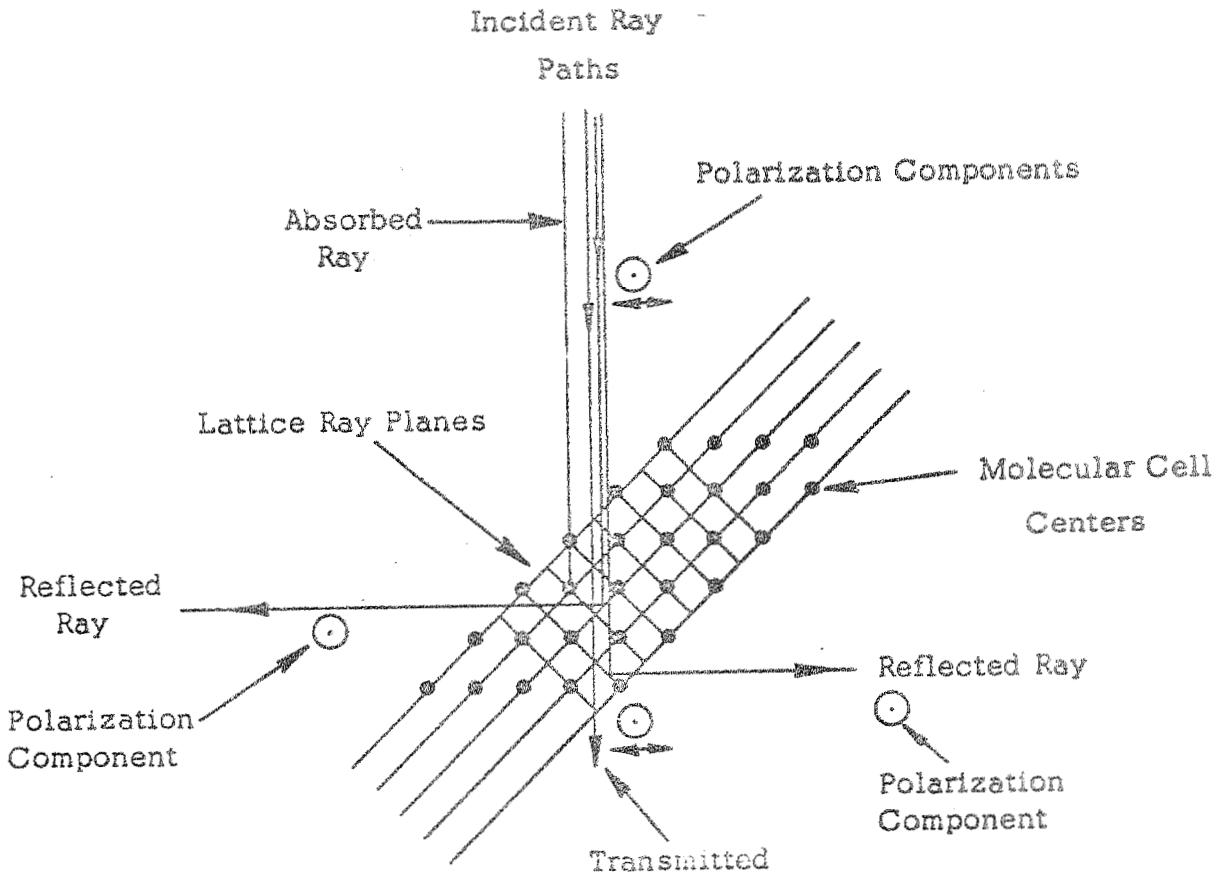

Figure 12. The LiH polarimeter crystal has cubic symmetry and therefore reflects the incident radiation in either of two directions

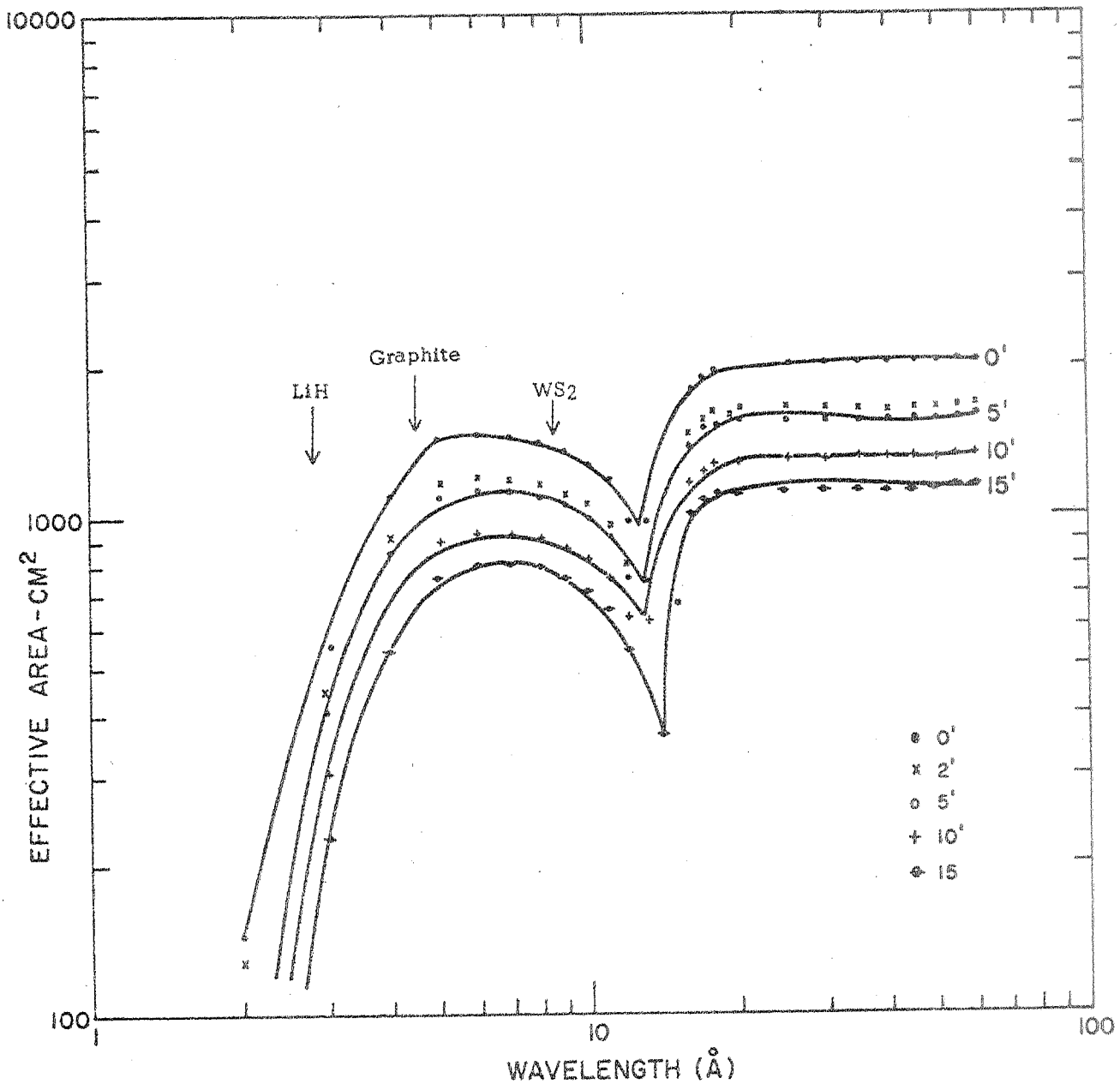

Figure 13. Effective area of high efficiency telescope with polarimeter energy samples indicated.

The theoretical and experimental sensitivities of these instruments to possible polarization of two stellar sources are summarized in Tables XV and XVI. The experimental estimates for graphite and lithium hydride are based on laboratory tests. We expect the sensitivity of the LiH to improve significantly toward the theoretical estimates. A conservative estimate of the experimental performance of the tungsten disulphide has been used. The effects of limited detector efficiency have been included in the experimental estimates.

We define the minimum detectable polarization P to be that value of polarization that has 1% probability of being exceeded in a measurement of an unpolarized source. We find, for example, that after a 1000-sec observation of the Crab nebula, the minimum detectable polarizations are 7.2%, 6.7%, and 5% for the tungsten disulphide, graphite, and lithium hydride polarimeters, respectively.

No background effects were included in the above estimates. The background results from cosmic-ray-induced events which simulate true x-ray events, and also from the fraction of the isotropic x-ray background which is collected by the telescope and then reflected into the detectors. Our own experience has been that by using anticoincidence and rise-time rejection schemes to reduce the cosmic-ray background, the remaining spurious events have the appearance of a spectrum with roughly a constant number of counts per keV of bandwidth of about 0.003 cts/cm^2/keV/sec. Comparison with other observations (Gorenstein et al., 1968) shows that rates even lower than the above value may be possible. With a maximum total area of order 100 cm^2 for any one of the polarimeters, and a conservative estimate of a one-keV bandwidth, we see from Table XVI that these experiments will only begin to be background-limited for sources ten times

Table XVI

Sensitivity to Polarization from the Crab Nebula:
Polarimeters at the Focus of the High Efficiency Telescope

A) Theoretical Estimates:

Material	Energy	Integrated intensity	Source flux	Effective area of telescope	R_{Th}	R^{*}_{Th}	Minimum detectable Polarization P
	(kev)	(X 10^4)	(kev/kev cm^2 sec)	(cm^2)	(cts/sec)	(cts/sec)	(%)
WS_2	1.41	16	7.0	1100	12.3	24.6	2.7
C	2.62	11	3.5	1250	4.8	9.6	4.3
LiM	4.30	35	2.2	900	6.9	27.7	2.5

B) Current Experimental Estimates

Material	Energy	Integrated intensity	Source flux	Effective area of telescope	R_{exp}	R^{*}_{exp}	R^{**}_{exp}	Minimum detectable Polarization P
	(kev)	(X 10^4)	(kev/kev cm^2 sec)		(cts/sec)	(cts/sec)	(cts/sec)	(%)
WS_2	1.41	10	7.0	1100	7.7	11.6	6.9	7.2
C	2.62	10	3.5	1250	4.4	6.6	3.9	6.7
LiM	4.30	20	2.2	000	4.0	11.9	7.1	5.0

Legend:

R = Number of counts/sec reflected from a thick crystal.

R^{*}_{Th} = R X 2 for WS_2 and C, X 4 for LiM to account for improvement in integrated intensity by the stacking and cleavage techniques.

R^{*}_{exp} = R X 1.5 for WS_2 and C, X 3 for LiM.

R^{**}_{exp} = 0.6 R^{*} for C and LiM and 0.33 X R^{*} for WS_2 to account for detector efficiency.

P = 3 standard deviations for a 1,000 sec observation.

Table XVII

Sensitivity to Polarization from Scorpius X-1
Polarimeters at the Focus of the High Efficiency Telescope

A) Theoretical Estimates:

Material	Energy	Integrated intensity	Source flux	Effective area of telescope	R_{Th}	R^{*}_{Th}	Minimum detectable Polarization P
	(kev)	(X 10^4)	(kev/kev cm^2 sec)	(cm^2)	(cts/sec)	(cts/sec)	(%)
WS_2	1.41	16	42	1100	74	148	1.1
C	2.62	11	33	1250	45	91 (11,000)	1.4
LiH	4.30	35	24	900	76	302 (35,000)	0.8

B) Current Experimental Estimates:

Material	Energy	Integrated intensity	Source flux	Effective area of telescope	R_{exp}	R^{*}_{exp}	R^{**}_{exp}	Minimum detectable Polarization P
	(kev)	(X 10^4)	(kev/kev cm^2 sec)	(cm^2)	(cts/sec)	(cts/sec)	(cts/sec)	(%)
WS_2	1.41	10	42	1100	46	69	42	3.0
C	2.62	10	33	1250	41	62	37	2.2
LiM	4.30	20	24	900	43	130	78	1.5

Legend:

R = Number of counts/sec reflected from a thick crystal.

R^{*}_{Th} = R X 2 for WS_2 and C, X 4 for LiM to account for improvement in integrated intensity by the stacking and cleavage techniques.

R^{*}_{exp} = R X 1.5 for WS_2 and C, X 3 for LiM.

R^{**}_{exp} = 0.6 R^{*} for C and LiM and 0.33 X R^{*} for WS_2 to account for detector efficiency.

P = 3 standard deviations for a 1,000 sec observation.

weaker than the Crab nebula. Even at this level, the counting rate from the isotropic background will be negligible.

D. An Imaging Polarimeter

An extended source such as the Crab nebula is of special interest for polarization measurements. A polarization map of such objects can be carried out most efficiently by locating a plane-reflecting crystal just before the focus of a high-resolution lens as shown in Fig. 14. An image will still be formed, and the polarization of different regions from the source can be measured simultaneously. An x-ray image intensifier can be conveniently used as the detection device for this experiment.

As an example of the resolution of such a device, we consider an image of the Crab nebula formed by an x-ray lens of one-arc-sec resolution. The image would be approximately 1/4 in. in diameter. A graphite crystal with a mosaic spread of 0.5° located 1/2 in. from the focal plane would give an image resolved to 4 arc sec.

Unfortunately, the requirement that a single plane surface be used for the imaging polarimeter eliminates the use of the previously described techniques for improving the integrated intensity of the crystal. The low efficiency of an x-ray image intensifier further limits the sensitivity of the experiment and would reduce the overall efficiency of the polarimeter by a factor of 16.

In comparison with the non-imaging polarimeters, we see from Table XV, for example, that a 4-hour measurement will be required to achieve equal sensitivity to polarization for the Crab nebula. If an image of this source is formed of n elements, an observation approximately n times as long will be required to obtain the same sensitivity to polarization in

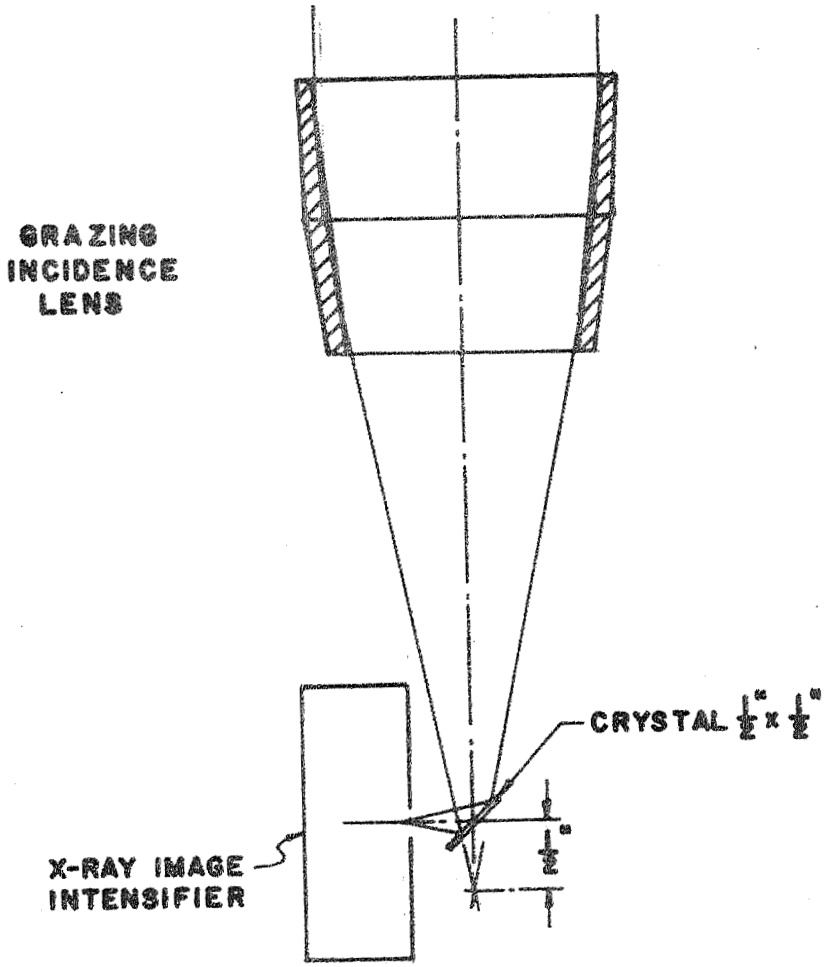

Figure 14. Imaging x-ray polarimeter concept.

each resolution element. Nevertheless, such an experiment would yield significant results because the two obvious sources of interest (the Crab nebula and M-87) are of sufficient intensity so that the reduced sensitivity will not result in unreasonably long integration times. For example, we will be able to detect 6% polarization from the Crab nebula as a three-standard-deviation effect in each of 6 spatial resolution elements in 24 hours of observation.

V. THE FOCUSING CRYSTAL POLARIMETER

We have currently completed preparing for flight the most sensitive x-ray polarimeter to date. This polarimeter will be used to search for polarization in the 2-3 keV range of the continuous emission from the Crab nebula. The polarimeter involves the use of over 900 square inches of graphite crystals and employs the strong polarization dependence of Bragg reflection at and near 45° reflection.

For the purpose of this report, the main feature of interest is the preparation of the crystals. Because of the large area of crystals involved and the high cost of the better grades of the material, special techniques were developed in order to produce the appropriate crystals for the polarization experiments.

Fortunately, high resolution (narrow mosaic spread) is not a prime requirement for these experiments as one is only interested in reflecting as much of the continuum as possible. A technique has been developed for producing a large number of crystals of the highest integrated intensity from a single square inch of the very poor quality (mosaic spread 3.5°) graphite crystals. This technique makes use of the fact that only a few thousand atomic layers of the material contribute to the

reflected intensity and the fact that one can peel off extremely thin (< 0.001 in.) layers from the crystal through the use of an adhesive tape. The process involves peeling several strips of crystal in such a manner that minute striations appear in the material. This perturbation seems to break up the large domains characteristic of these crystals as evidenced by the high integrated reflectivity of the finished product. Several thin layers are then cold-welded together at a pressure of approximately 2000 lbs/sq in. The resulting crystal shows typically an integrated intensity of better than 8×10^{-4} at 2.6 keV or almost 90% of the theoretically predicted value. A typical rocking curve for these crystals is shown in Fig. 15.

The rocket containing these crystals (NASA Flight 17.09 UG) was flown successfully on February 21, 1971. The results of this flight will be sent as an appendix to this report as they become available.

GRAPHITE CRYSTALS #A653-5 (X RAY ENERGY = 2.53 KEV)

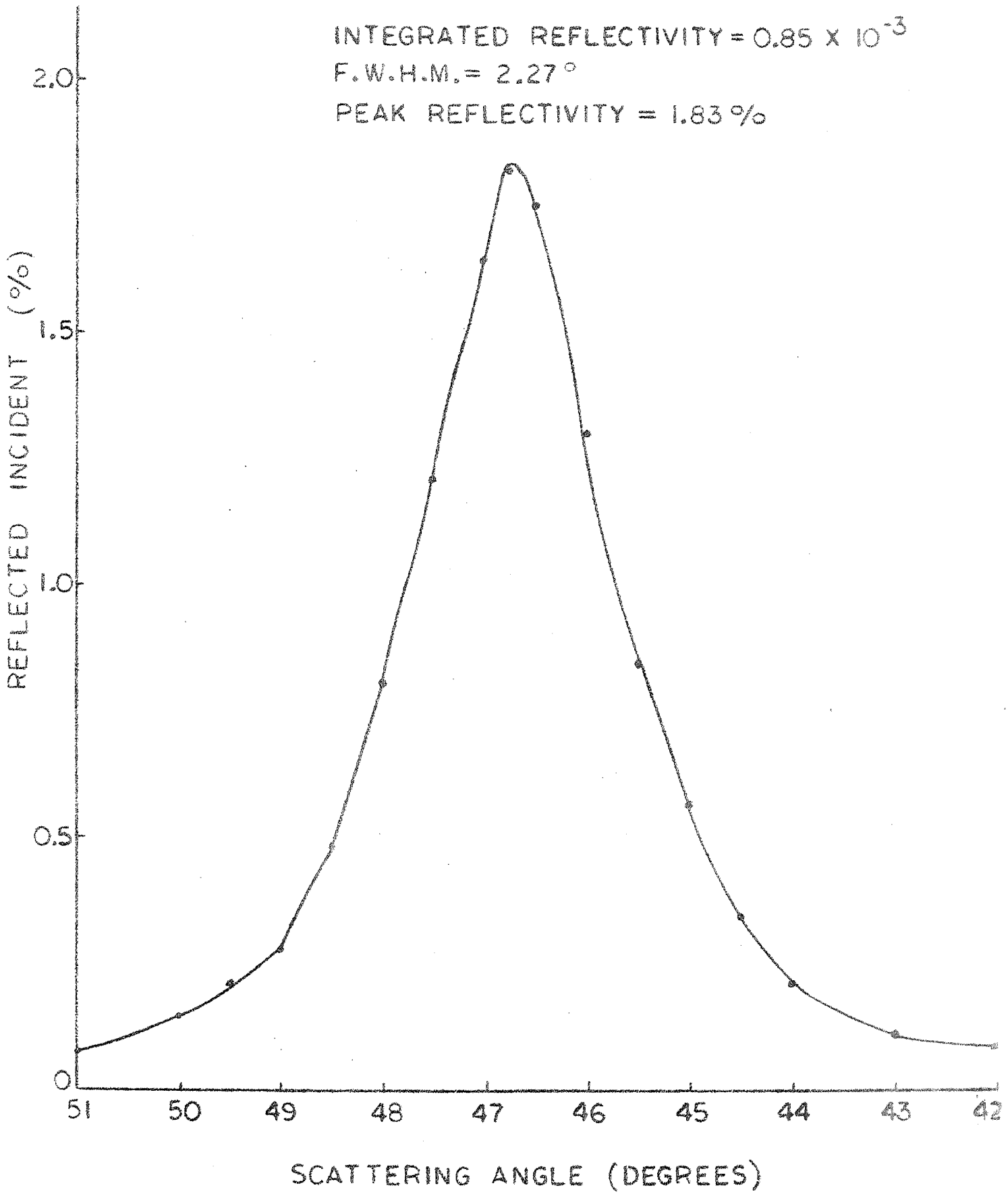

FIGURE 15